Fermi National Accelerator Laboratory

FERMILAB-TM-1958

Hadron Calorimeter Performance with a PbWO4 EM Compartment

Dan Green

Fermi National Accelerator Laboratory
P.O. Box 500, Batavia, Illinois 60510

January 1996

Operated by Universities Research Association Inc. under Contract No. DE-AC02-76CHO3000 with the United States Department of Energy

Fermi National Accelerator Lab
Compact Muon Solenoid
December 15, 1995

TM-1958

Hadron Calorimeter Performance with a PbWO4 EM Compartment

Dan Green
Fermilab

Introduction

The CMS detector[1] at the LHC has chosen PbWO4 in order to achieve the superior photon energy resolution which is crucial in searching for the 2 photon decay of low mass Higgs bosons. The hadronic compartment is thought to be Cu absorber, since one is immersed in a 4 T magnetic field, read out by scintillator tiles coupled to wavelength shifter (WLS) fibers. The combined performance of this calorimeter is of interest in the study of jets and missing transverse energy (neutrino, SUSY signatures).

For this reason, a test was made of the electromagnetic (EM) compartment combined with a reasonable approximation to the baseline HCAL "barrel" calorimeter. Data was taken in the H4 CERN beamline. The EM compartment was a 7x7 square array of PbWO4 crystals, which for the purposes of this study are considered as a single readout in depth (or "compartment") [2]. The HCAL module consisted of large scintillator plates with 24 individual longitudinal readout channels. The EM compartment was followed by 10 Cu plates each 3 cm thick, followed by 9 Cu plates each 6 cm thick. This set of absorber plates represented the HCAL compartments inside the coil. The coil itself [1] was approximated as Al and Fe plates, of a total thickness of about 1.4 absorption lengths. The coil mockup was sampled and then followed by 4 plates of 8 cm thick Cu, each with an individual readout which represented a test of the "Tailcatcher" concept.

This full calorimeter array of 25 longitudinal samples was exposed to beams of muons, electrons, and pions of different energies. The muon beam exposures were used to establish a minimum ionizing particle calibration. Using this calibration, and the sampling thickness of Cu, the energy profile shown in Fig. 1 was obtained with the test module exposed to 375 GeV negatively charged pions. Note that the full stack is about 10 absorption lengths deep. The quality of the muon calibration can be seen in that the curve is continuous.[3] Hadron shower maximum occurs at a depth of about 2 absorption lengths.

The "Tail catcher" Compartment

Any real calorimeter is of finite length, and thus subject to leakage of energy due to incomplete containment. In CMS the current baseline is to use the first part of the magnet return yoke steel, 25 cm thick, as additional absorber, in order to minimize energy leakage. The test beam stack was then partitioned into 4 "compartments" in order to approximate the baseline CMS calorimeter. The first section is the crystal EM compartment. The next 2 independent readouts are called h1 and h2 which are partitions of the samples (2 to 20 in Fig. 1) inside the coil. The sampling outside the coil consists of 2 coarse (~ 1.5 Lambda) samples, the first directly following the coil (sample 21 in Fig. 1) and the second right after the return steel (roughly approximated by sample 24 in Fig. 1), added together to become the h3 compartment.

These 4 compartments and sample 20 were allowed to have independent weights. The baseline HCAL design is to have independent readout of EM, h1, h2, and h3 (the tail catcher) and allow a passive weighting of sample 20 using thicker plastic or more WLS fibers. As will be discussed later, the relative weights of these readouts was adjusted so as to minimize the energy resolution at a fixed energy (375 GeV was used here). This weighting was subsequently applied to all events and to all energies.

Having adopted this scheme for relative weighting of the 4 "compartments" of the calorimeter, the utility of the "tailcatcher" compartment, h3, could then be evaluated. Shown in Fig.2 is the correlation between the energy measured inside the CMS coil, Eem+h1+h2, and the energy measured in the tail catcher, Eh3, normalized to the nominal beam energy Eo. In Eh2 is included the energy of the sample, weighted optimally, directly before the coil, sample 20. One notes that there is a strong correlation, at 375 GeV, of the 2 energies. It is also important to note that of the 1000 events plotted, there are ~ 10, or 0.1%, where more than 30% of the beam energy appears in the h3 compartment. Clearly, this compartment is needed in order to suppress rare leakage events which would mimic events with large missing energy.

It should not be thought that this is simply a case of very high energy leakage. Shown in Fig.3 is a plot of energy in the h3 compartment vs energy inside the coil for 50 GeV incident pions. Although the device resolution is poorer in this case than in Fig. 2, still there is a correlation, and h3 can be used to reduce the effects of leakage. It is worth noting that exp(-6.5) or 0.0015 of all pions simply fail to interact in the EM+h1+h2 compartments, independent of energy. A plot of the fraction of the incident energy appearing in the h3 compartment as a function of beam energy, E_o, is shown in Fig.4. Note the ln(E) behavior, which is expected in the case of the tails of hadronic showers. Note also that the rms of the h3 energy is observed to be > the mean. Thus a CMS calorimeter without h3 would suffer ~ 5% energy resolution at 500 GeV due to leakage alone. The h3 compartment, therefore, allows one both to reduce the effects of catastrophic energy mismeasurement and to improve the rms energy resolution of high energy hadrons.

Optimal Weighting of the Compartments

The energy measurement for 375 GeV incident pions was optimized using a sample of 1000 events. First events where > 1.2 times the beam energy appearing in the EM compartment were removed, leaving 993 events. The rms/mean, dE/E, of the energy distribution for muon calibration was 9.2%. Next the partition of h1/h2 was chosen so as to optimize the energy resolution. Surprisingly, the optimal location of the h1/h2 boundary was quite soft. However, there was a distinct preference for a short h1 compartment. The optimal boundary occurred for a 6 cm Cu h1, or only a few Xo. One suspects that this observation is related to the fact that the crystal EM compartment is quite noncompensating. It is not ruled out, however, that there is transverse shower leakage since the crystal EM array and the Cu HCAL array were spatially distinct, as in the CMS baseline [1].

With this partition, the weights of the compartments were 0.9 -EM, 1.46 -h1, 0.97 - h2, 0.985-h3, and 1.64 - layer 20. The weights are all roughly those obtained from muon calibration except for h1 and sample 20. In the case of sample 20, one expects that one should overweight late developing showers which exit ito the coil, and that effect is indeed observed. In the case of h1, one might expect that one should overweight the electromagnetic part of the showers which begin in EM, which also appears to be called for. The rms/mean is then 8.55%. A fit to a gaussian peak with polynomial background yields a rms/mean of 7.3%. The energy distributions for 375 GeV incident pions for muon calibration and for optimal weighting are shown in Fig.5. One can see a general reduction in the width of the distribution and a reductions of the non-Gaussian tails with the imposition of optimal weighting. Note also that with the fine sampling longitudinally available in this device we can sort on the beginning of the shower. It is found that the resolution is 6.9 % for events beginning in HCAL, but 8.9% for events initiated in ECAL. This effect may indicate that the crystal detector is rather strongly noncompensating. However, transverse leakage in the small EM crystal array cannot be completely ruled out.

Resolution, e/pi, and Noncompensation

Data were analyzed for 375, 120, 50, 25, and 15 GeV incident negative pion beams. A scatterplot of the energy in the EM compartment vs the energy in the HAD compartments is shown in Fig. 6 for 375 GeV pions. The optimal weight strategy means that the energy resolution was minimized subject to the constraint that the mean energy was the nominal beam energy. Thus, in Fig. 6 one expects the data to lie along the line shown which indicates the response of a linear device. An similar plot for 120 GeV is shown in Fig. 7 and for 25 GeV is shown in Fig. 8. In both cases the weights used were energy independent, having been established in the case of 375 GeV incident pions. Note the developing nonlinearity of the composite calorimeter as the energy decreases.

The ratio of energy deposited in the EM compartment to that deposited in h1+h2 is shown in Fig. 9. Clearly, low energy hadrons preferentially deposit their energy in EM, while higher energy hadron showers extend deeper into the HCAL. This effect contributes to the observed energy dependence of the device nonlinearity. The observed rms/mean at the 5 energies is shown in Fig. 10. The x axis is 1/E while the y axis is (rms/mean)^2 or (dE/E)^2. On such a plot a detector which can be characterized by a "stochastic" and a "constant" term added in quadrature will appear to be linear. This behavior is roughly observed, as indicated by the dashed line in Fig. 10. The stochastic term is 134%, while the constant term is 4.8%, i.e. dE/E = $a/\sqrt{E} \oplus$ b, a = 1.34, b = 0.048. If fits to gaussian peaks plus polynomial background are made, then a= 1.25 and b= 0.034.

In order to attempt to understand the behavior of the composite CMS calorimetry, a simple model was constructed. Hadrons were assumed to shower in ν generations. Each generation produced exactly <n> secondaries/primary with a fraction, fo=1/3, neutral. The neutrals were assumed to immediately drop out of the shower and deposit their energy , E_o.[4] This simple minded model results in the number of charged, $n_\pm(\nu)$, and neutral, $n_o(\nu)$, particles, the energy/particle and the deposited neutral energy, E_o at different depths/generations as shown in Table. 1.

The cascade continues to develop until more pions cannot be made, at threshold energy Et.

$$\begin{aligned} &1/\langle n\rangle^{\nu_{\max}} = E_T / E \\ &E_T \sim 2m_\pi \end{aligned} \tag{1}$$

Clearly, at that maximum depth/generation, ν max a fraction Fo of the initial energy has beendeposited by neutrals. Clearly, at low energies Fo --> fo since there is only 1 generation. For very high energies, vmax is large, and thus Fo --> 1.

$$\begin{aligned} &F_o = f_o \sum_{\nu=1}^{\nu_{\max}} (1-f_o)^{\nu-1} \\ &\rightarrow f_o[(1-f_o)^{\nu_{\max}-1} - 1]/[\ln(1-f_o)] \end{aligned} \tag{2}$$

In an attempt to smooth out the discrete nature of the model, as would occur for example if n was not <n>, or if generations did not occur at fixed depths, one converts the expression for Fo from a sum, ν, to an integral in Eq.2.

Suppose that one has a simple homogeneous detector, without compartments. If the response of the detector to electrons/photons, e, was not the same as the response to hadrons, h (called noncompensation), then the energy recorded for electrons E_e would differ from that recorded for pions E_π.

$$
\begin{aligned}
E_\pi &= eF_o + h(1-F_o) \\
E_e &= e \\
e/\pi &= \frac{(e/h)}{[(e/h)F_o + (1-F_o)]}
\end{aligned}
\tag{3}
$$

The e/pi ratio then depends on e/h and Fo. Clearly, for Fo = 1 (high energies) the ratio --> 1 since the detected energy in the hadron cascade is all electromagnetic.

The fact that e/h is not = 1 means that an hadronic shower will be mismeasured because of fluctuations in the total neutral content, dFo.

$$
\begin{aligned}
dE_\pi &= (e-h)dF_o \\
\frac{dE}{E} &\sim \frac{dF_o|e/h-1|}{[(e/h)F_o + (1-F_o)]}
\end{aligned}
\tag{4}
$$

The fractional energy error , dE/E, depends on e/h, Fo, and dFo. If e/h=1, then there is no contribution due to the fluctuations dFo. Suppose the fluctuations in the neutral content, dfo, of any interaction are Gaussianly distributed. If one assumes that dfo/fo = dFo/Fo, then the fractional error due to these fluctuations is related to dE/E.

$$
\begin{aligned}
f_o &= \langle n_o \rangle / \langle n \rangle \\
df_o / f_o &= 1/\sqrt{f_o \langle n \rangle} \\
dE/E &= \frac{df_o (F_o/f_o)|e/h-1|}{[(e/h)F_o + (1-F_o)]}
\end{aligned}
\tag{5}
$$

Clearly, for low energies, Fo --> fo, and, very approximately, dE/E --> dfo|e/h-1|. Numerically, dE/E ~ 0.3|e/h-1|.

In the context of this simple model, vmax as a function of E is shown in Fig. 11. The slow increase of vmax from 1 at low energy is evident, reaching 3.5 at 1 TeV. The neutral fraction, Fo, as a function of E is given in Fig. 12. Both the discrete and the continuous versions (Eq.2) are displayed. At low energies, Fo --> fo = 1/3, while at very high energies, Fo --> 1. The rise is slow, however, reaching only 53% at 100 GeV. Using Fo as shown in Fig. 12, one can generate dE/E and e/pi for different values of e/h. The values of dE/E shown in Fig. 13 are roughly constant with energy. For example, e/h=1.2 leads to a 6% "constant term" due to noncompensation. The e/pi values are given in Fig. 14. There is only a weak energy dependence above ~ 200 GeV. However, the rapid rise of Fo with energy means that e/pi rises rapidly with decreasing E at low energies. For example, with e/h = 1.4, e/pi ~ 1.15 at E = 100 GeV.

The rms/mean, dE/E for the 5 energies studied is shown in Fig. 15. The data points are both for fixed weights, independent of energy and for weighting reoptimized at each energy and with interactions only in the HCAL compartments. For all interaction points, whether or not one uses energy independent optimal weights has only minor impact. What is important is whether or not the hadron begins to shower in the EM compartment. The 2 data sets shown in Fig. 15 can be roughly represented as possessing stochastic terms of 136% and 79% and constant terms of 4.8% and 6% for interactions anywhere or in the HCAL compartment respectively. If fits to gaussian peaks with quadratic background are perfomed in the former case, the resolution appears to be improved. The stochastic term is 125% and the constant term is 3.4%. Clearly, the composite ECAL + HCAL behaves worse than a simple Cu/scintillator HCAL acting as a stand alone device. Note that as mentioned before, the effects of transverse leakage cannot be unscrambled, in this dataset, from the effect of non-compensation. There is also a longitudinal nonuniformaty in the ECAL crystals which will contribute adversely to the energy resolution.

One can infer that the effective e/h of the composite is substantial. Using the points shown in Fig. 13, a constant term of ~ 8% means an effective e/h of ~ 1.3. The curve plotted in Fig. 15 is the dE/E due to e/h=1.3 folded in quadrature with a 100% stochastic term. That curve roughly describes the data over the energy range spanned by the data. The e/pi ratio is another indication of the effective e/h of the device. The e/pi is extracted by assigning e to be the nominal beam energy - assuming that the EM compartment is a linear device and that the nominal beam energy is correct. The pi value is extracted from the mean response when energy independent weights determined from 375 GeV data are used. That method effectively defines e/pi = 1 at 375 GeV. The resulting e/pi values at the 5 energies are shown in Fig. 16. The e/pi value falls with increasing energy as ln(E) from a value ~ 1.26 at E=15 GeV. Looking at Fig. 14, a variation of e/pi by ~ 0.26 from 15 to 375 GeV occurs only for rather high values of e/h.

Clearly, other experimental biases must be studied before one can make a strong conclusion about the effective value of e/h based on e/pi. One can also note that e/h is itself energy dependent [5]. Therefore, a rather more sophisticated model should be invoked before conclusions are reached. One can, however, note that a Pb-Fe composite device (SDC) had a substantial e/pi variation in this energy range [6]. Note also that a highly noncompensating device such as a Cerenkov sensitive quartz fiber "spaghetti" device has a 40% variation in e/pi over the same energy range [7]. Therefore, the presently observed e/pi ratio reported in Fig. 16 is not totally implausible. More analysis is in progress in order to sharpen the discussion.

References:

1. The Compact Muon Solenoid, Technical Proposal, CERN/LHCC 94-38, December 15, 1994.

2. We thank our colleagues of the CMS ECAL group for their help in taking this data set.

3. The CMS HCAL group was responsible for collecting this interesting data set.

4. Dan Green, "Selected topics in sampling calorimetry" FN-607, Fermilab (1993).
D. Green, EM Clusters in Hadron Showers using the "Hanging File" Data, Fermilab FN-612 (1993).

5. R. Wigmans, advances in Hadron Calorimetry, Ann. Rev. Nuc. Part. Sci. 41 133 (1991).

6. Solenoid Detector Collaboration, Technical Design Report SDC-92-201 (1992)

7. L. Sulak, private communication.

Figure Captions:

Fig. 1 Profile of the calorimeter exposed to 375 GeV pions. The first point is the EM compartment. The HCAL consists of 10 layers of 3 cm Cu sampling, followed by 9 layers of 6 cm sampling, followed by a mockup of the CMS coil, followed by 8 cm Cu sampling in the "tail catcher". The 25 independent longitudinal readouts were calibrated using a muon beam and using sampling fraction weighting.

Fig. 2 Scatter plot of the energy observed inside the CMS coil, Eem+h1+h2 vs the energy observed in the "tail catcher" Eh3. The straight line indicates a linear correlation. The data are from a 375 GeV pion exposure.

Fig. 3 Same as Fig. 2 save that the data are from a 50 GeV pion exposure.

Fig. 4 The fraction of incident energy, Eo, seen in the "tail catcher" as a function of Eo. The line is drawn simply to guide the eye and indicate the ln(Eo) behavior of Etc/Eo=Eh3/Eo.

Fig.5 Total energy distribution in the calorimeter as exposed to 375 GeV pions. a. Using muon calibration as indicated by the profile in Fig. 1. b. Using "optimal weight", meaning minimizing the energy resolution by adjusting the relative weight of the 5 compartments.

Fig. 6 Scatter plot of Eem vs Ehad for 375 GeV incident pions and optimal weighting. The line indicates the response of a linear device with perfect resolution.

Fig. 7 As in Fig. 6 except that the weighting is that appropriate to 375 GeV while the data are from a 120 GeV pion exposure.

Fig. 8 As in Fig. 6 except that the weighting is that appropriate to 375 GeV while the data are from a 25 GeV pion exposure.

Fig. 9 The ratio of Eem to Eh1+h2 as a function of incident energy Eo. The line is included simply to guide the eye.

Fig. 10 Plot of the (rms/mean) squared, (dE/E)^2, as a function of the inverse of the incident energy 1/Eo. The dashed line indicates the behavior of a calorimeter characterized by a "stochastic" term and a "constant" term.

Fig. 11 The maximum number of hadronic generations vmax as a function of the incident hadron energy, E.

Fig. 12 Energy dependence of the effective neutral fraction Fo. The smooth curve is the integral representation of the discrete sum shown as a series of step functions.

Fig. 13 The contribution to the fractional energy resolution, dE/E, due to non- compensation as a function of incident hadron energy, E, for e/h = 1.0 (dE=0), 1.2, 1.4, 1.6 and 1.8.

Fig. 14 The energy dependence of e/pi for e/h = 1.0 (e/pi=1), 1.2, 1.4, 1.6 and 1.8.

Fig. 15 The energy dependence of the data, shown as o, for the calorimeter energy resolution, dE/E, using weighting defined by optimizing the resolution at 375 GeV. The curve corresponds to the folding in quadrature of a 110% stochastic term with the contribution due to e/h=1.3. The data, shown as •, refers to events initiated in the HCAL and with optimal weighting performed independently at each energy.

Fig. 16 The energy dependence of the data for the e/pi ratio using weighting defined by optimizing the resolution at 375 GeV. It is assumed that the e response of the EM compartment is linear, so that the beam energy can be used to define e.

TABLE 1

Model for Hadron Showers

v	$\varepsilon(v)/E$	$n(v)$	$n_o(v)$	E_o/E
0	1	1	0	0
1	$1/\langle n \rangle$	$(1-f_o)\langle n \rangle$	$f_o\langle n \rangle$	f_o
2	$1/\langle n \rangle^2$	$(1-f_o)^2\langle n \rangle^2$	$(1-f_o)\, f_o\langle n \rangle^2$	$f_o(1-f_o)$
3	$1/\langle n \rangle^3$	$(1-f_o)^3\langle n \rangle^3$	$(1-f_o)^2\, f_o\langle n \rangle^3$	$f_o(1-f_o)^2$

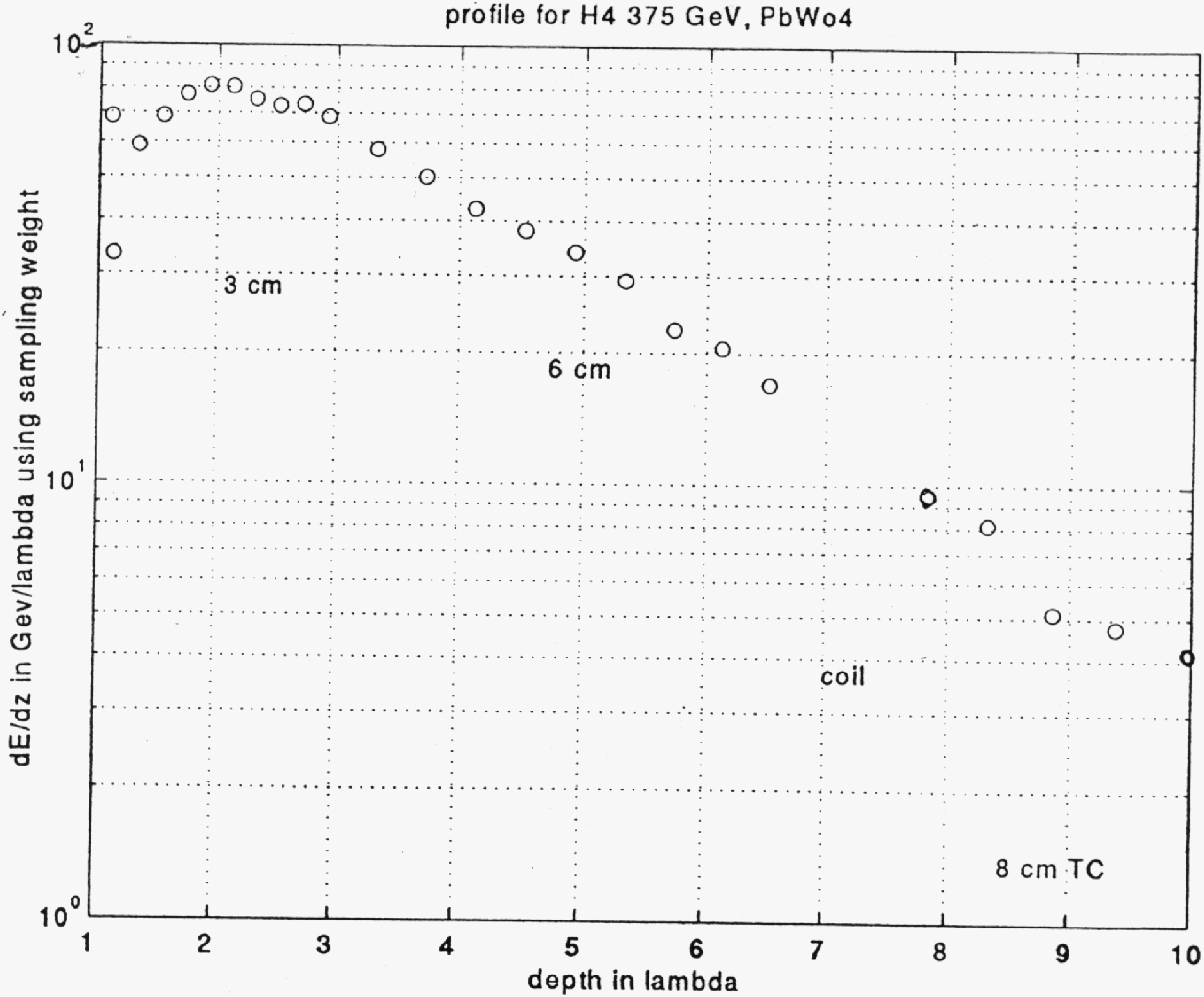
profile for H4 375 GeV, PbWo4
dE/dz in Gev/lambda using sampling weight
depth in lambda
3 cm
6 cm
coil
8 cm TC
10^2
10^1
10^0
1
2
3
4
5
6
7
8
9
10

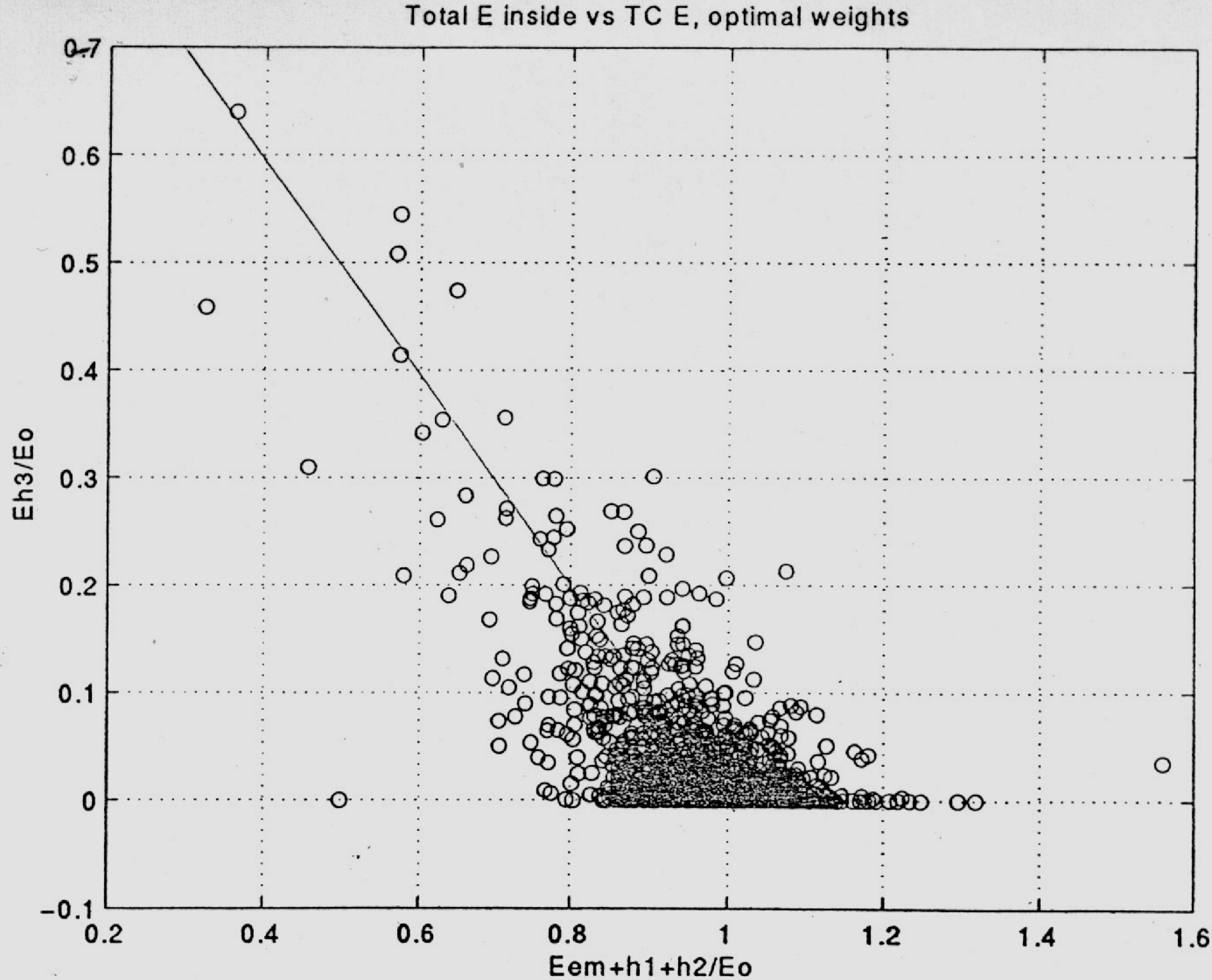
Total E inside vs TC E, optimal weights
Eh3/Eo
Eem+h1+h2/Eo
0.7
0.6
0.5
0.4
0.3
0.2
0.1
0
−0.1
0.2
0.4
0.6
0.8
1
1.2
1.4
1.6

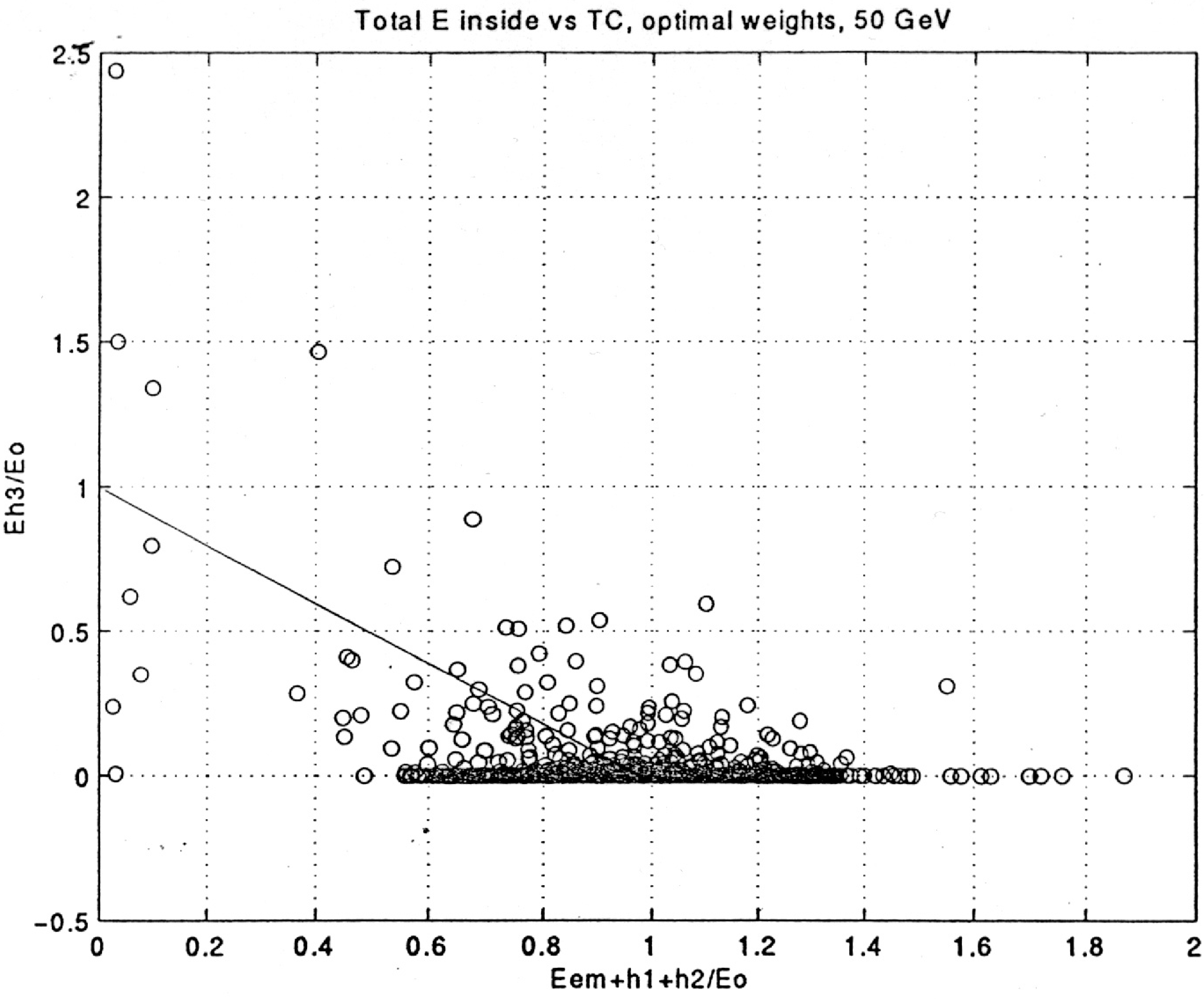
Total E inside vs TC, optimal weights, 50 GeV
Eh3/Eo
Eem+h1+h2/Eo
2.5
2
1.5
1
0.5
0
-0.5
0
0.2
0.4
0.6
0.8
1
1.2
1.4
1.6
1.8
2

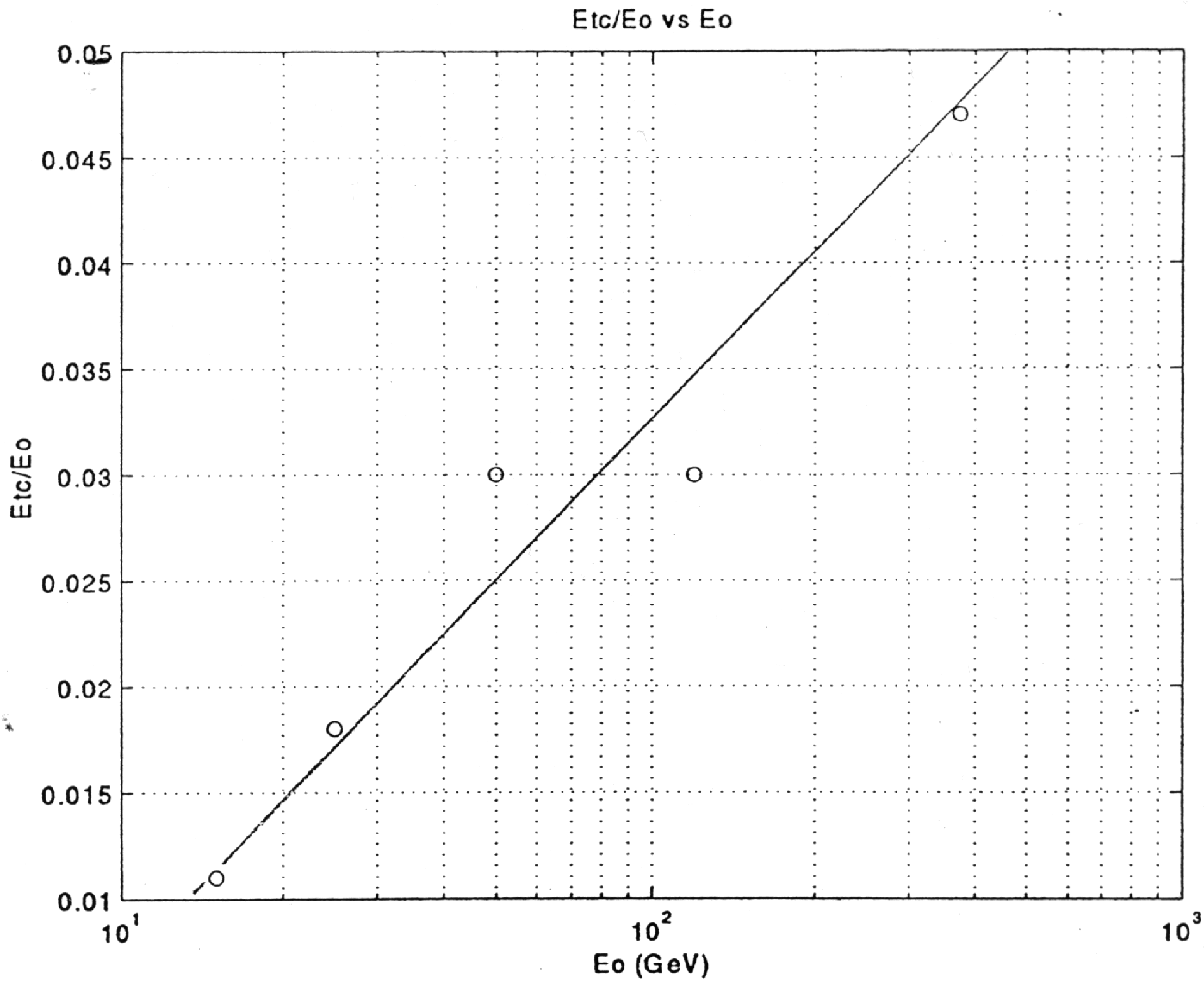

Etc/Eo vs Eo
0.05
0.045
0.04
0.035
0.03
0.025
0.02
0.015
0.01
Etc/Eo
10^1
10^2
10^3
Eo (GeV)

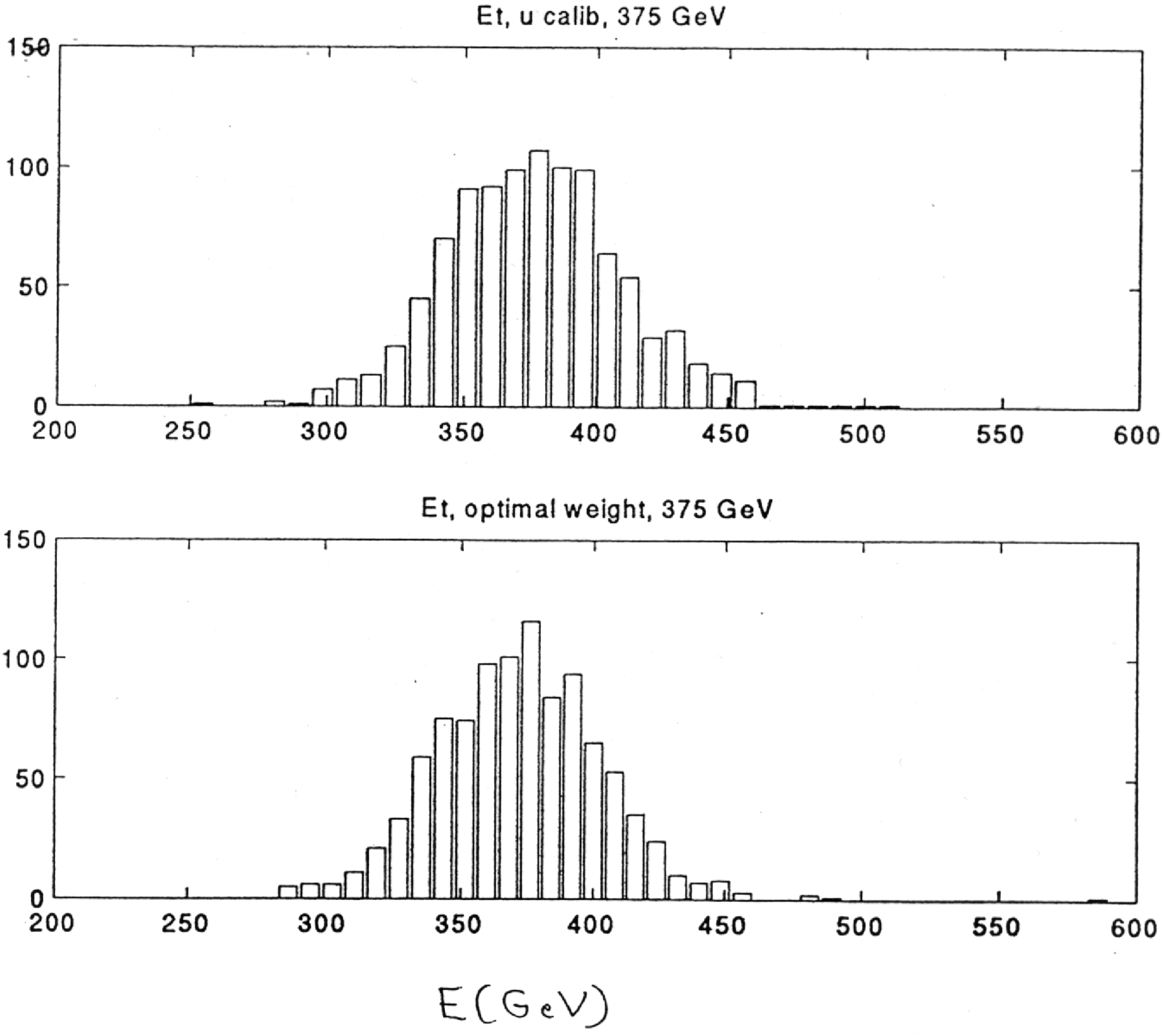
Et, u calib, 375 GeV
150
100
50
0
200
250
300
350
400
450
500
550
600
Et, optimal weight, 375 GeV
150
100
50
0
200
250
300
350
400
450
500
550
600
E(GeV)

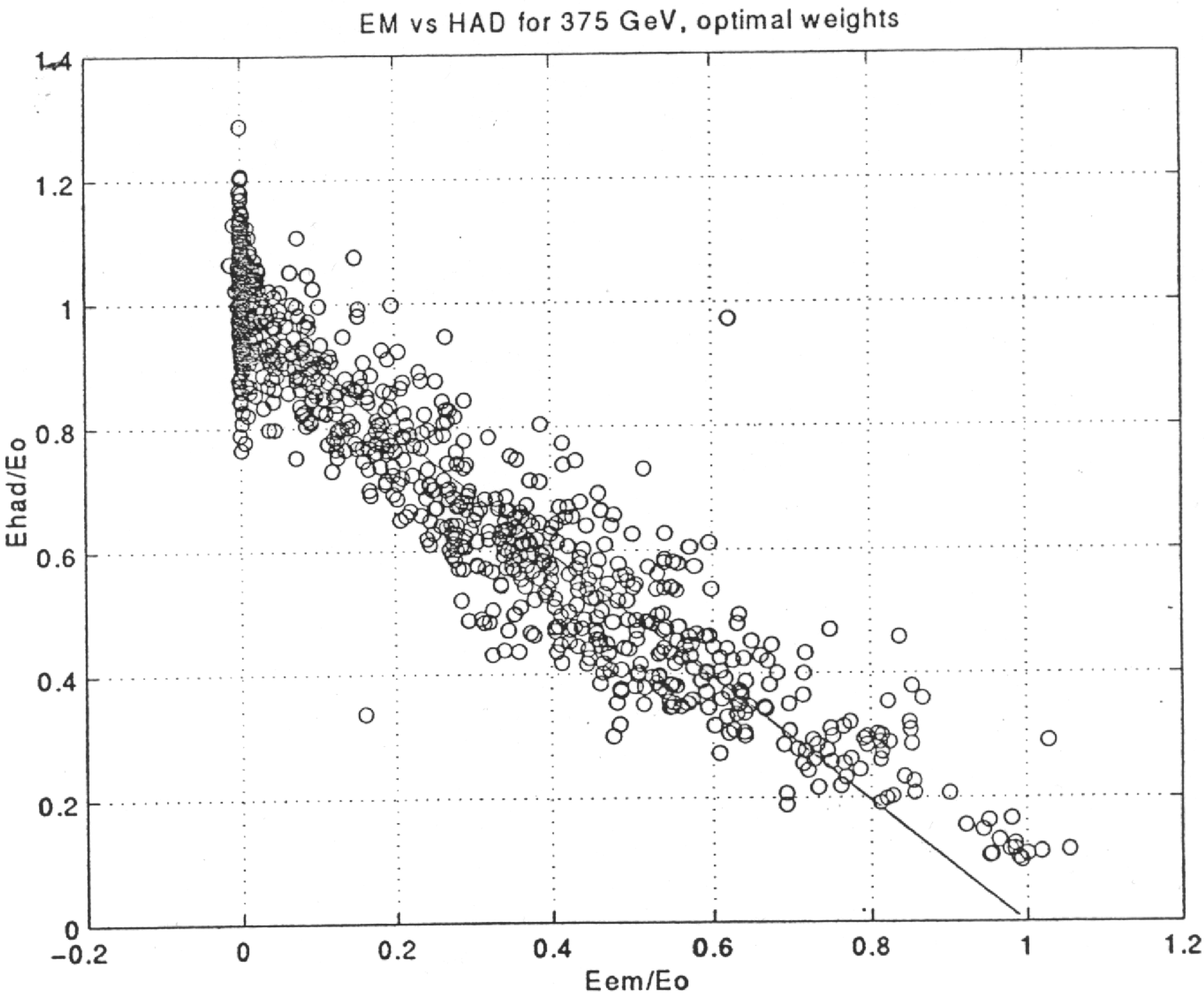

EM vs HAD for 375 GeV, optimal weights
1.4
1.2
1
0.8
0.6
0.4
0.2
0
Ehad/Eo
-0.2
0
0.2
0.4
0.6
0.8
1
1.2
Eem/Eo

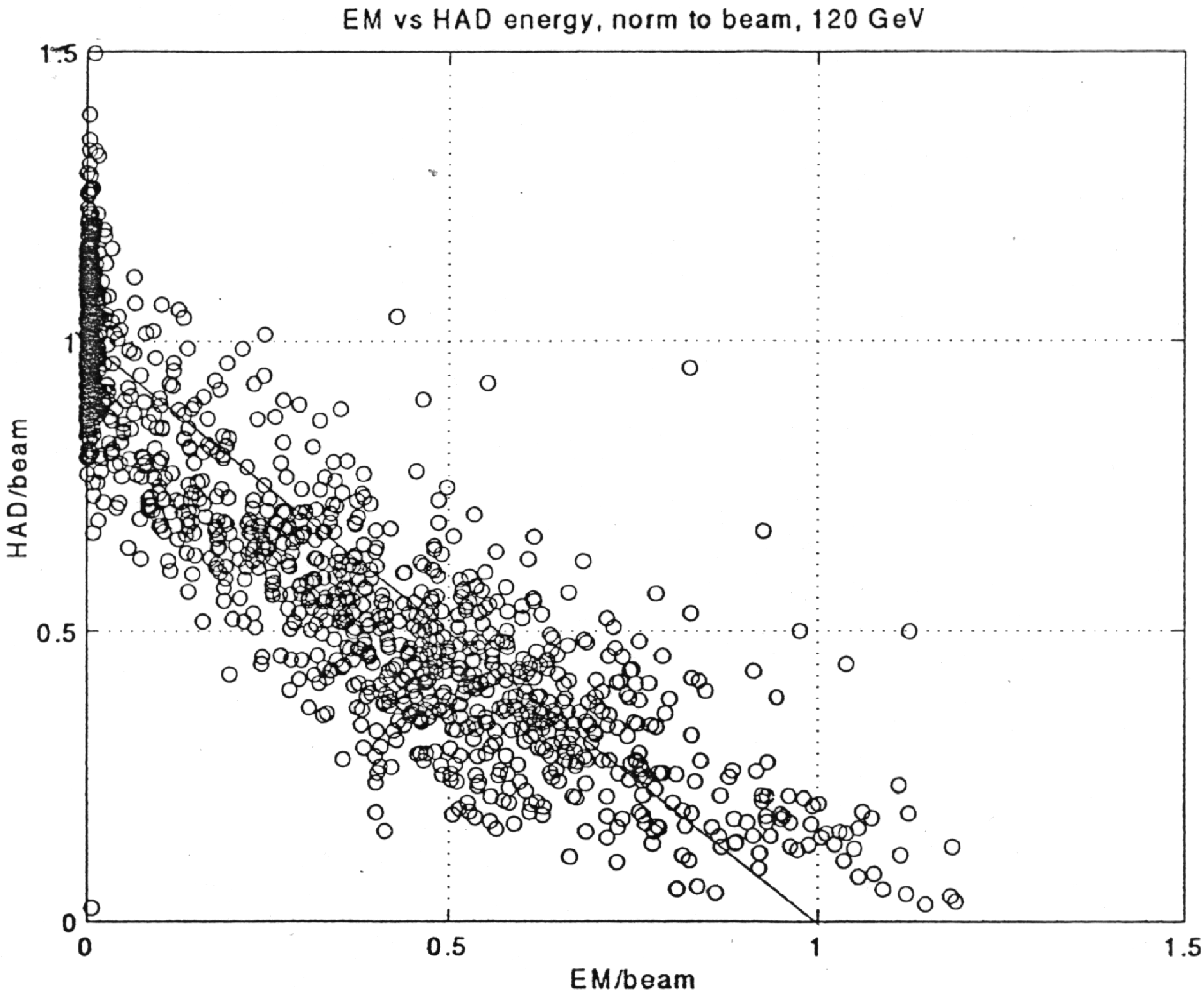
EM vs HAD energy, norm to beam, 120 GeV
HAD/beam
EM/beam
0
0.5
1
1.5
0
0.5
1
1.5

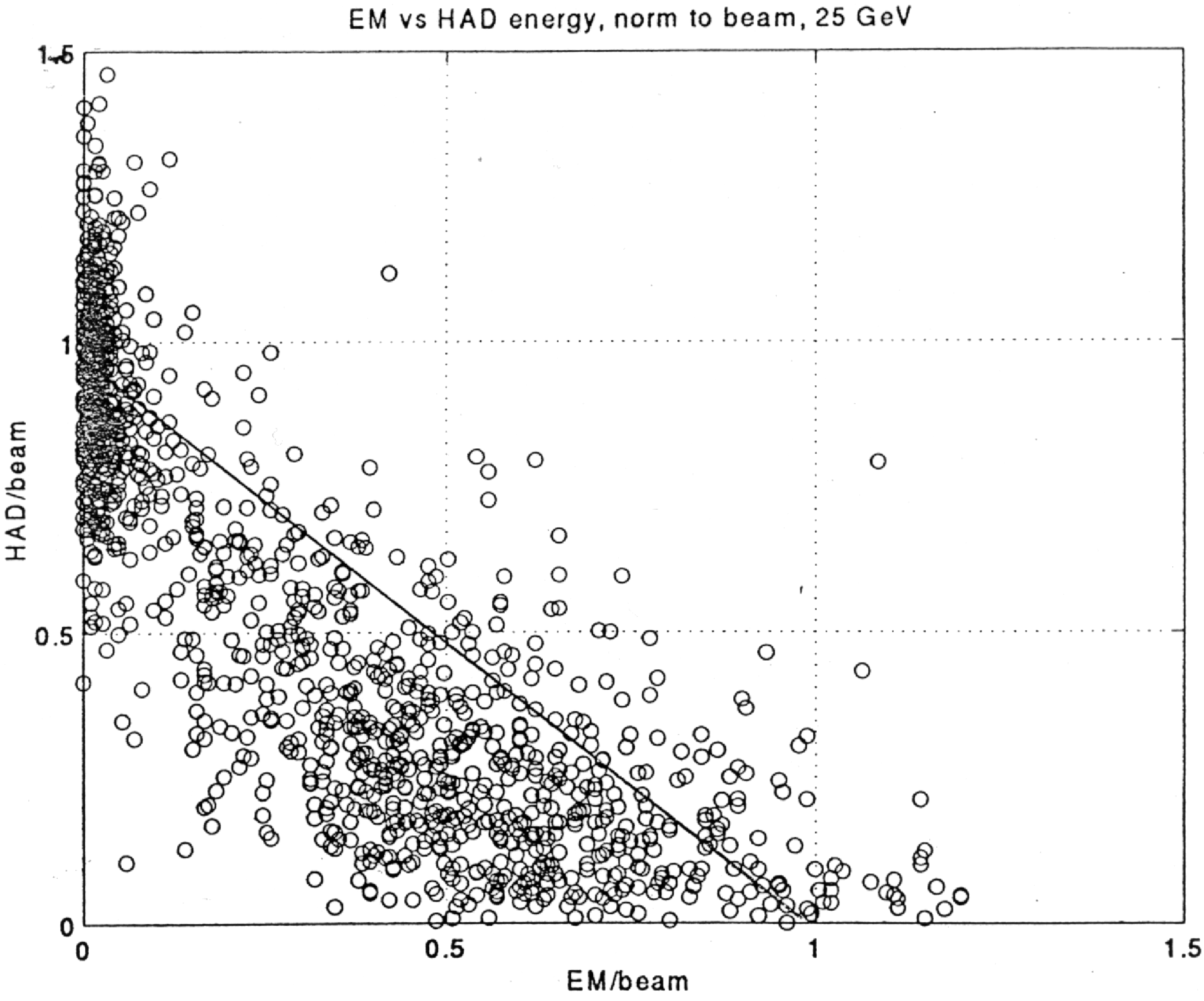
EM vs HAD energy, norm to beam, 25 GeV
HAD/beam
EM/beam
0
0.5
1
1.5

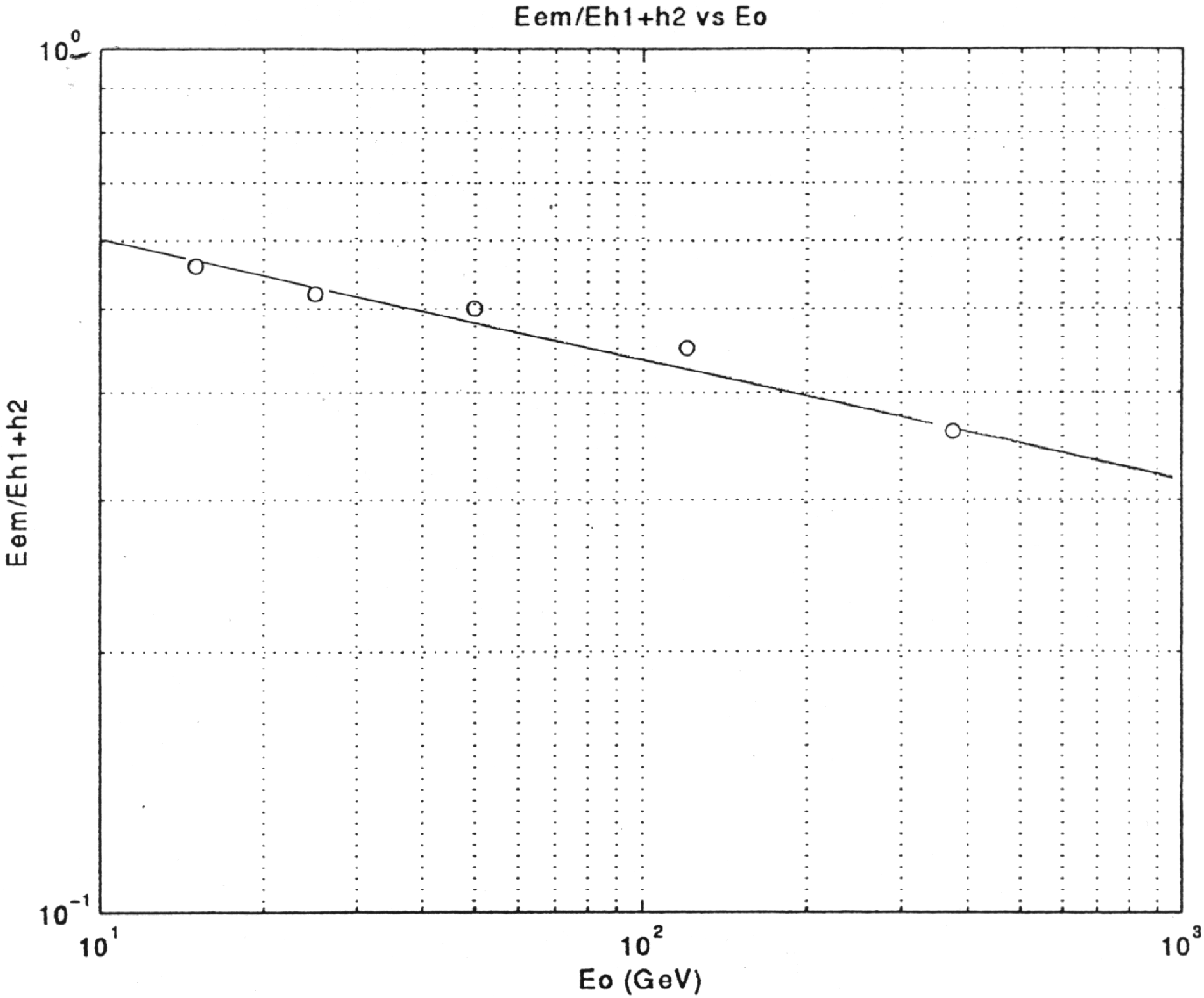

Eem/Eh1+h2 vs Eo
Eem/Eh1+h2
Eo (GeV)
10^0
10^{-1}
10^1
10^2
10^3

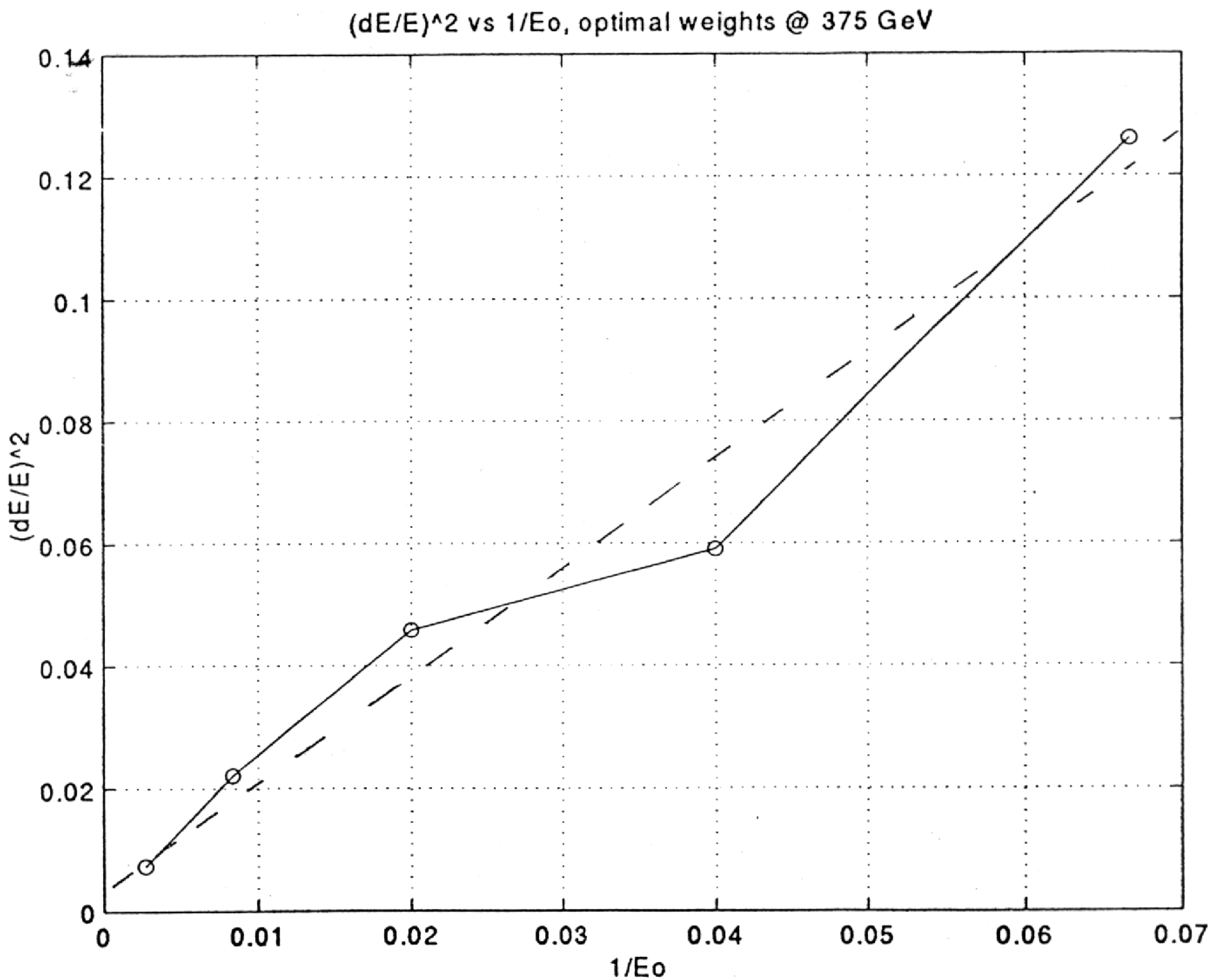

(dE/E)^2 vs 1/Eo, optimal weights @ 375 GeV
0.14
0.12
0.1
0.08
0.06
0.04
0.02
0
(dE/E)^2
0
0.01
0.02
0.03
0.04
0.05
0.06
0.07
1/Eo

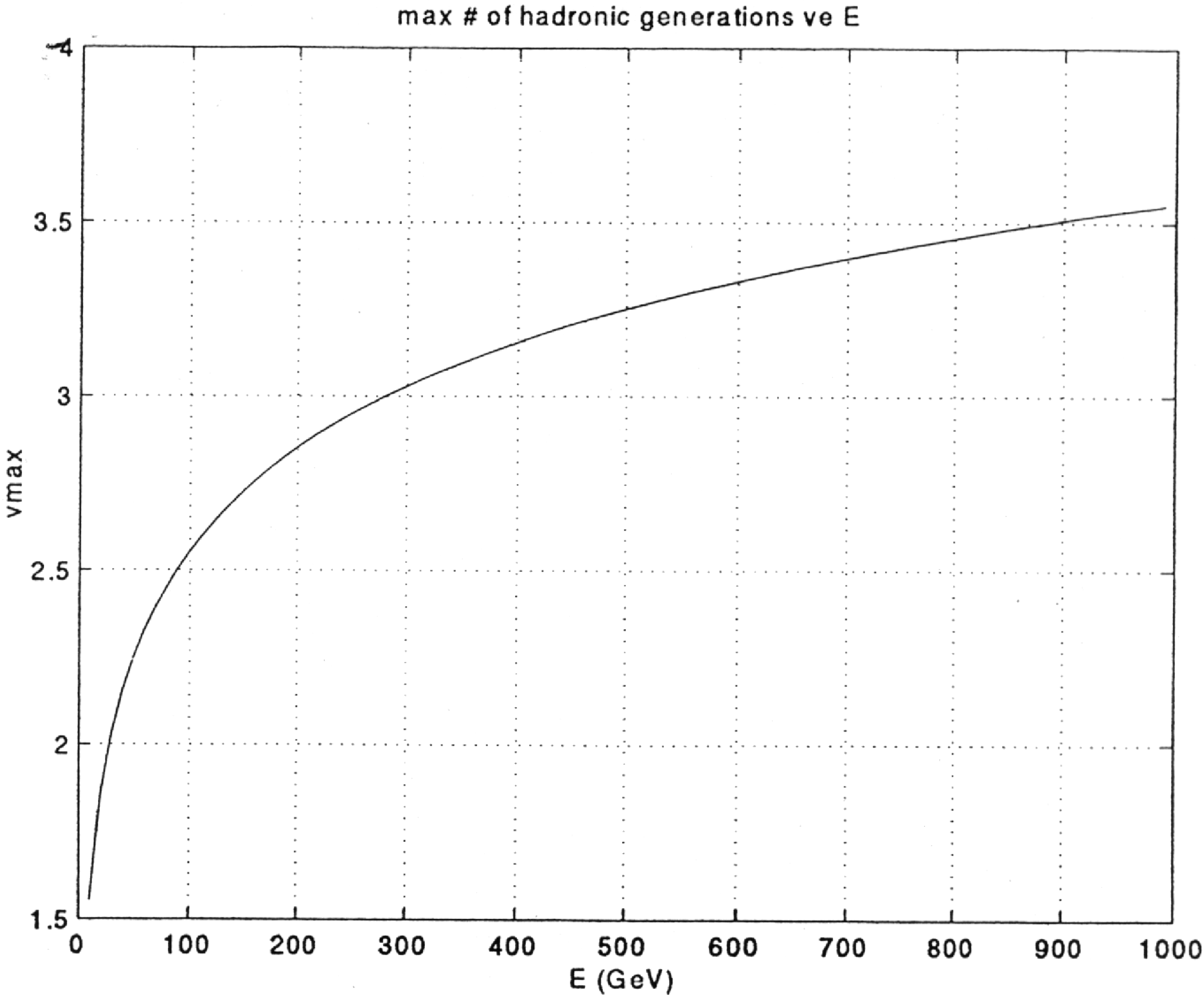
max # of hadronic generations ve E
vmax
4
3.5
3
2.5
2
1.5
0
100
200
300
400
500
600
700
800
900
1000
E (GeV)

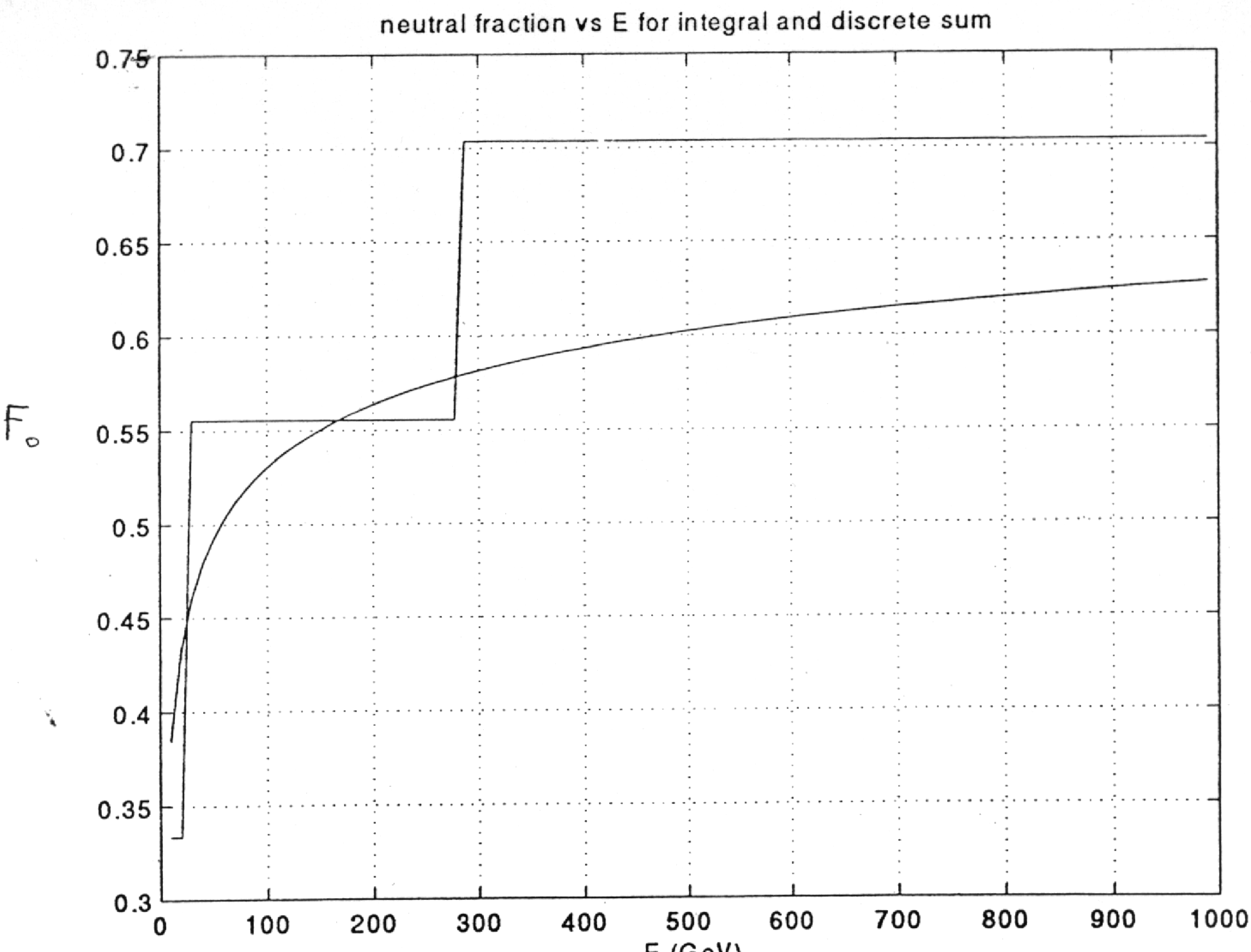

neutral fraction vs E for integral and discrete sum
F_0
E (GeV)
0.75
0.7
0.65
0.6
0.55
0.5
0.45
0.4
0.35
0.3
0
100
200
300
400
500
600
700
800
900
1000

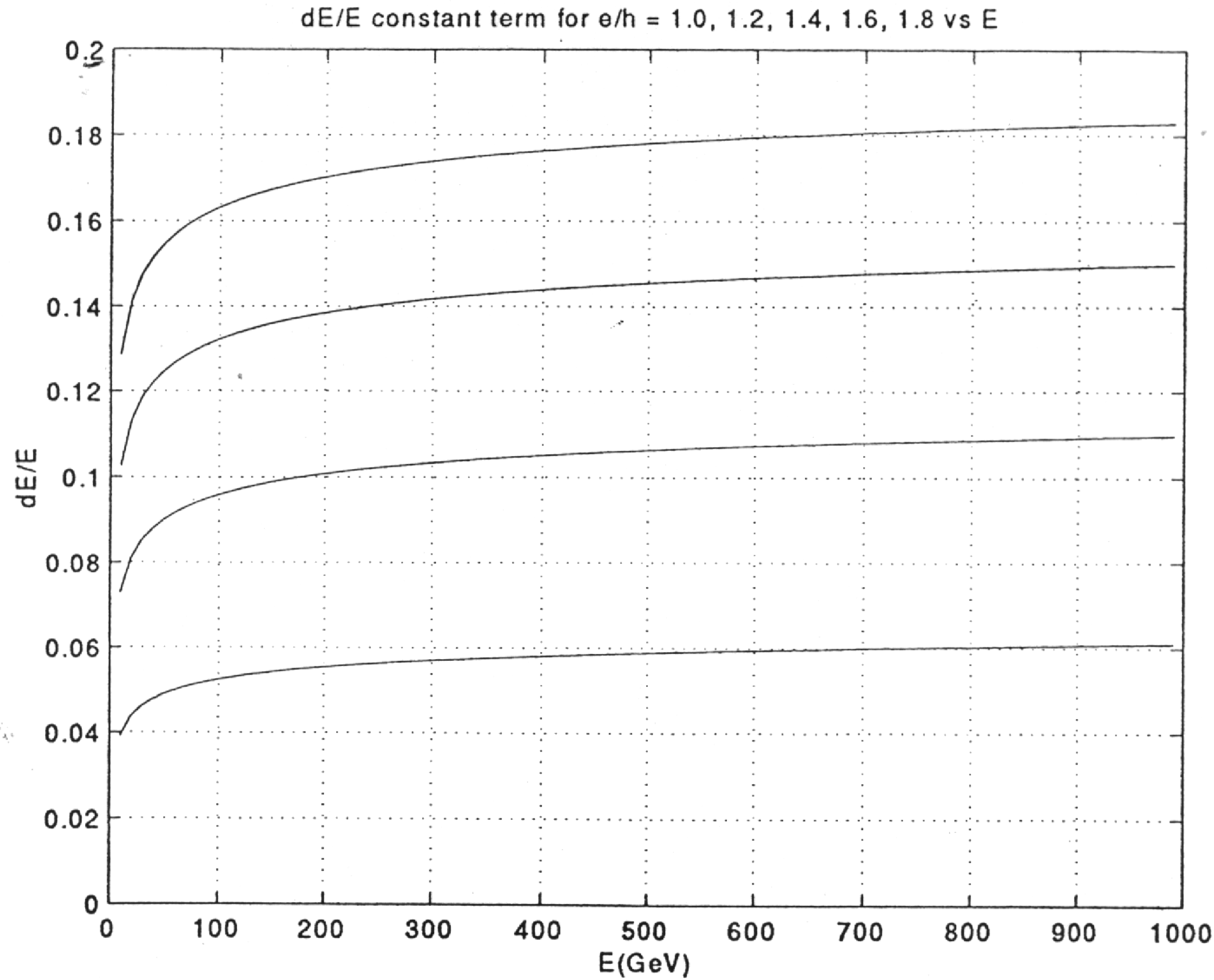
dE/E constant term for e/h = 1.0, 1.2, 1.4, 1.6, 1.8 vs E
dE/E
E(GeV)
0
0.02
0.04
0.06
0.08
0.1
0.12
0.14
0.16
0.18
0.2
0
100
200
300
400
500
600
700
800
900
1000

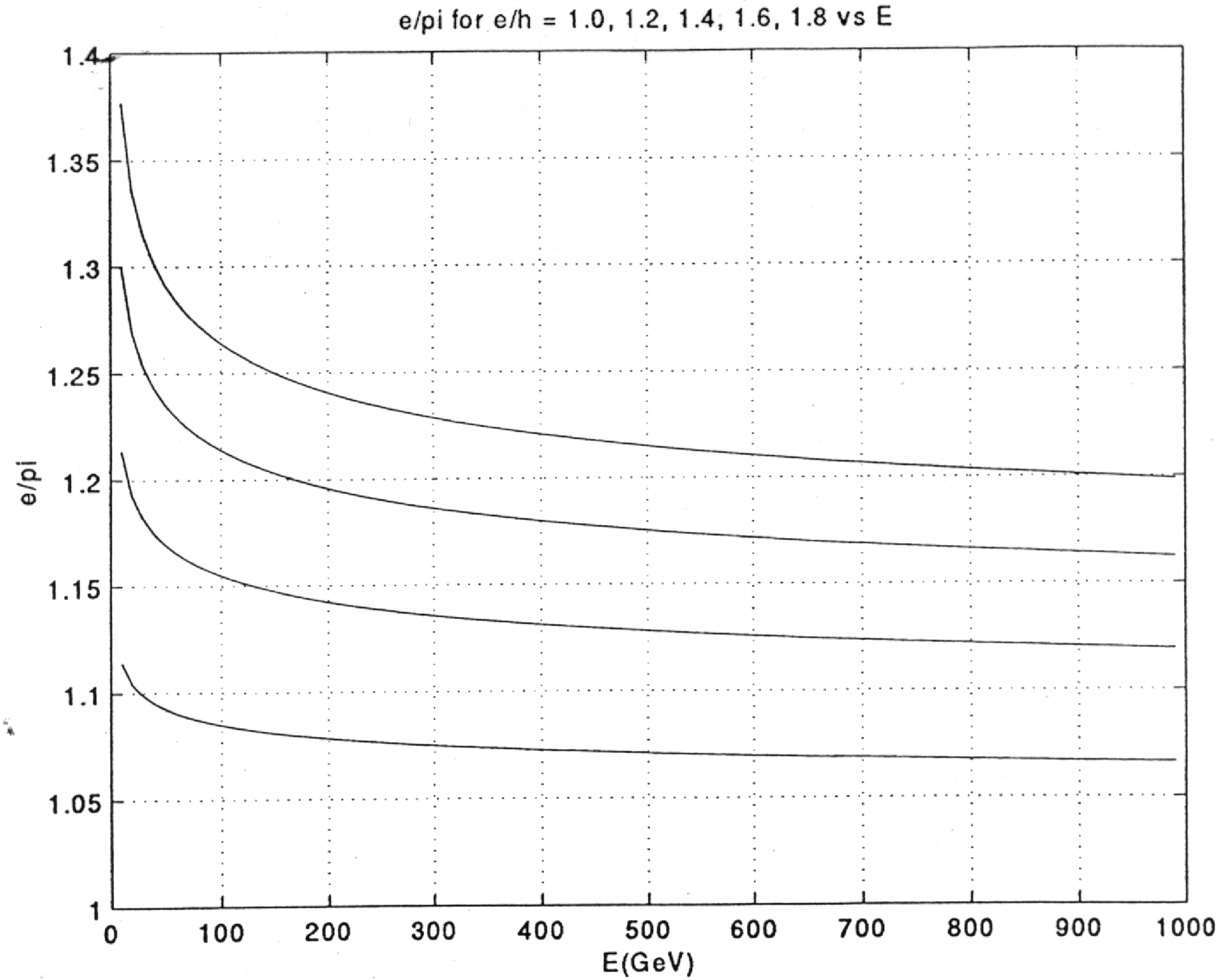

e/pi for e/h = 1.0, 1.2, 1.4, 1.6, 1.8 vs E
e/pi
1.4
1.35
1.3
1.25
1.2
1.15
1.1
1.05
1
0
100
200
300
400
500
600
700
800
900
1000
E(GeV)

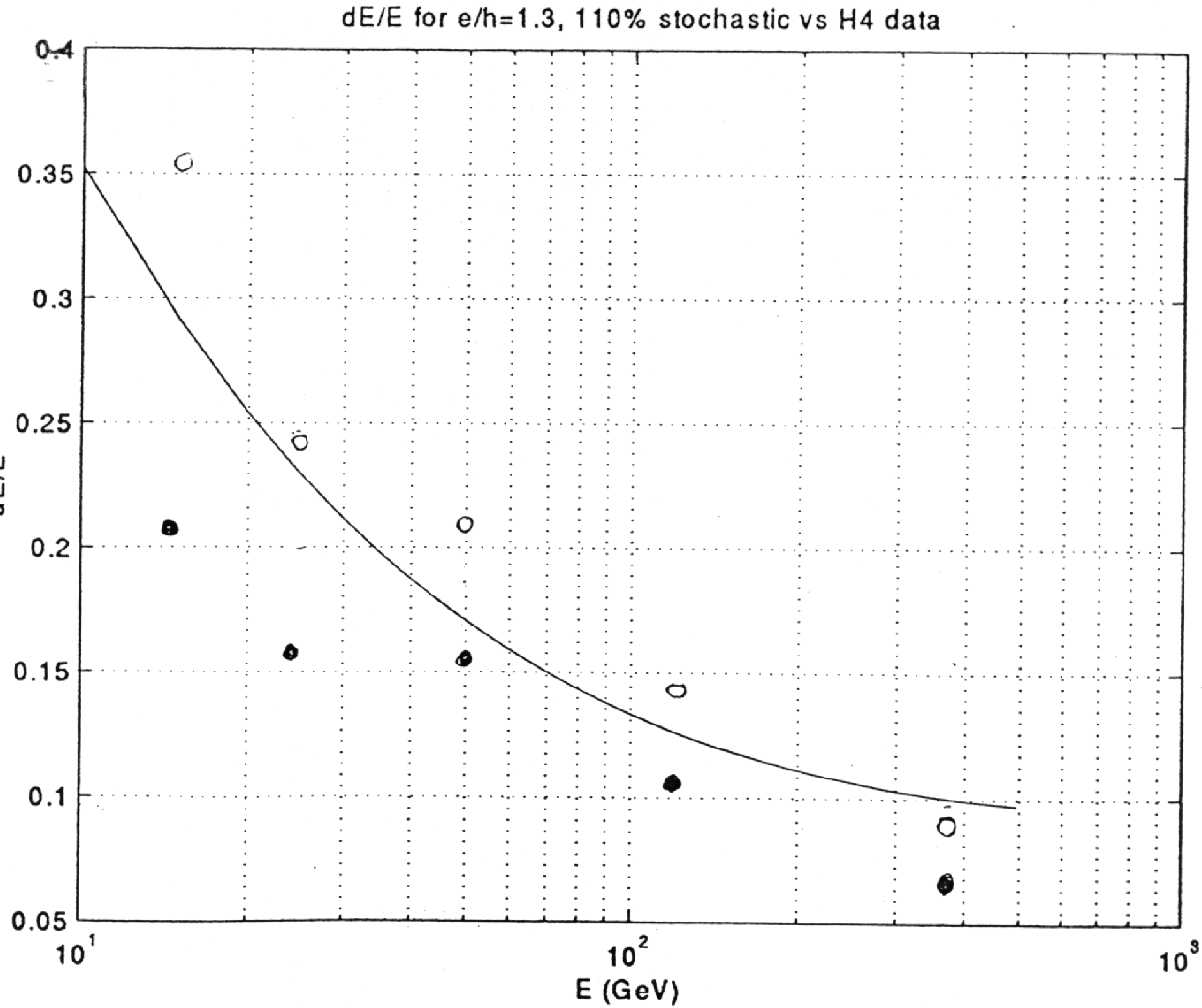
dE/E for e/h=1.3, 110% stochastic vs H4 data
dE/E
0.4
0.35
0.3
0.25
0.2
0.15
0.1
0.05
10^1
10^2
10^3
E (GeV)

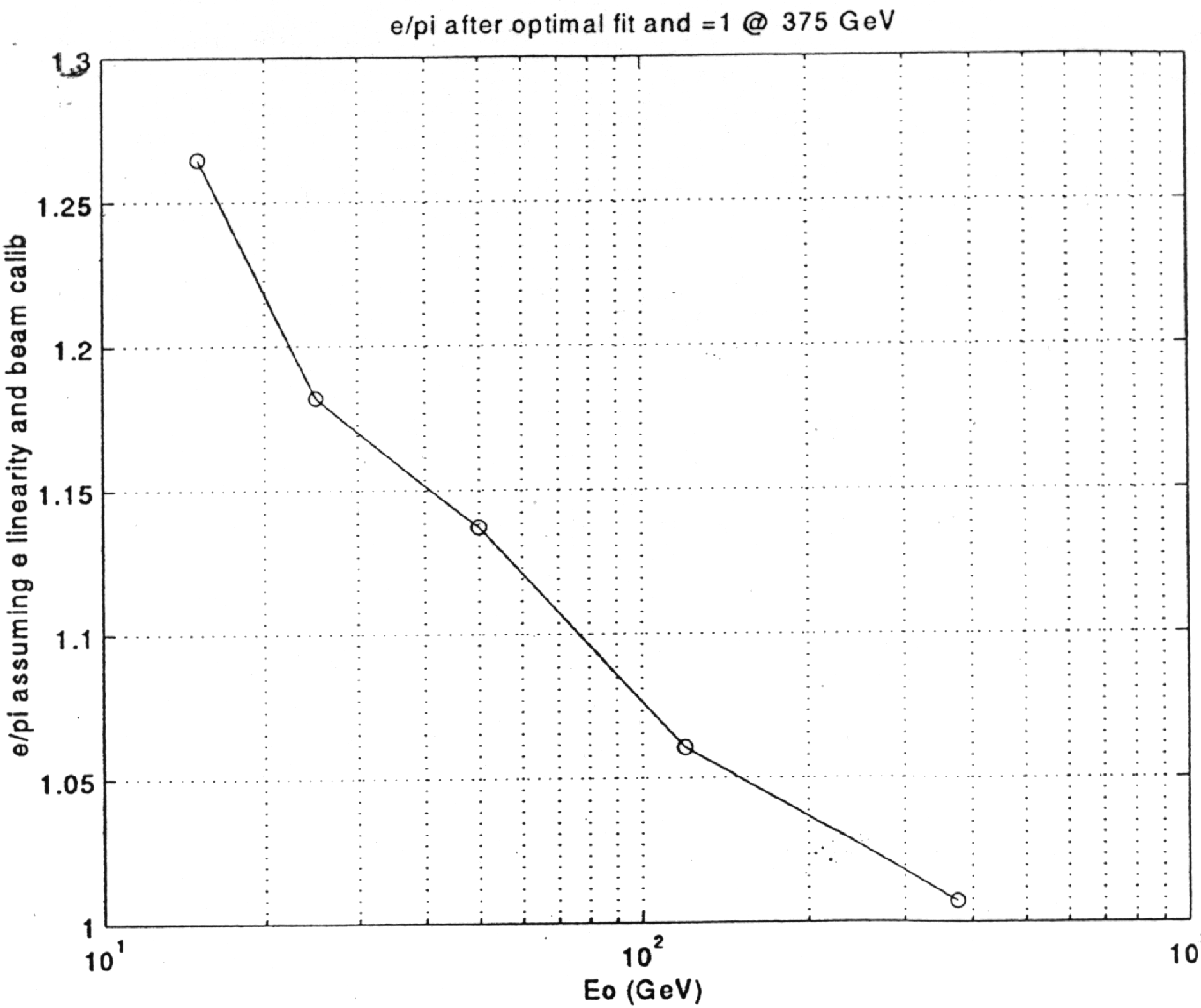

e/pi after optimal fit and =1 @ 375 GeV
1.3
1.25
1.2
1.15
1.1
1.05
1
e/pi assuming e linearity and beam calib
10^1
10^2
10^3
Eo (GeV)